J|A|C|S
A R T I C L E S

Zwitterionic Polymerization: A Kinetic Strategy for the Controlled Synthesis of Cyclic Polylactide

Wonhee Jeong,[†] Eun Ji Shin,[†] Darcy A. Culkin,[†,§] James L. Hedrick,[‡] and Robert M. Waymouth*,[†]

Department of Chemistry, Stanford University, Stanford, California 94305, and IBM Almaden Research Center, 650 Harry Road, California 95120

Received December 15, 2008; E-mail: waymouth@stanford.edu

Abstract: The zwitterionic ring-opening polymerization of lactide initiated by *N*-heterocyclic carbenes generates cyclic polylactides with well-defined molecular weights between $M_n = 5000$ and 30 000 g/mol with narrow polydispersities ($M_w/M_n \leq 1.31$). These zwitterionic polymerizations are extremely rapid ($k_p = 48.7\ M^{-1}\ s^{-1}$), but also exhibit exceptional control of molecular weight and molecular weight distribution. The unusual kinetic features of these zwitterionic polymerizations are illuminated with kinetic and mechanistic investigations, which implicate a mechanism that involves a slow initiation step (second order in [M]), a propagation step (first order in [M]) that is much faster than initiation ($k_i = 0.274\ M^{-2}\ s^{-1}$), cyclization ($k_c = 0.0575\ s^{-1}$), and depropagation ($k_d = 0.208\ s^{-1}$). Numerical and stochastic simulations of the kinetic data provide a kinetic rationale for the evolution of molecular weight with monomer conversion: the molecular weights increase with increasing monomer conversion, exhibit a nonzero intercept near 0% monomer conversion, and are relatively insensitive to the initial monomer-to-initiator ratio. The observed narrow molecular weight distributions are due to a high rate of propagation relative to cyclization and chain transfer. Kinetic simulations define the kinetic criteria under which the active zwitterions remain in solution; these simulations were substantiated by chain-extension experiments, which provide experimental evidence for chain extension of the zwitterions and reinitiation by the *N*-heterocyclic carbenes liberated upon macrocyclization. The kinetic model rationalizes some of the unique features of zwitterionic ring-opening polymerization and provides a useful mechanistic framework to optimize these polymerizations as a strategy to generate well-defined cyclic polyesters.

Introduction

Cyclic macromolecules have fascinated chemists, biologists, and materials scientists for decades.[1−3] The simple topological constraint of connecting the ends of a large linear macromolecule into a ring has a significant influence on the structure, dynamics, and properties of the polymer, but our understanding of the origin of these effects is only beginning to take shape.[1,4−7] The synthetic challenges in generating high molecular weight cyclic polymers are formidable as the unfavorable entropy of cyclization presents both thermodynamic and kinetic constraints for large chains.[8,9] Experimental efforts to generate large ring macromolecules typically involve the coupling of two reactive ends of a linear telechelic precursor at high dilutions,[1,2,5,10−14] or the use of polymeric supports.[15,16] More recently, ring expansion strategies[17] have been devised utilizing cyclic ruthenium[18−21] and cyclic tin alkoxide initiators[22] to generate high molecular weight cyclic polymers.

[†] Stanford University.

[‡] IBM Almaden Research Center.

[§] Current address: Ashland Performance Materials, 5200 Blazer Parkway, Dublin, OH 43017.

(1) Semlyen, J. A. *Cyclic Polymers*, 2nd ed.; Kluwer Academic Publishers: Dordrecht, 2000.
(2) Semlyen, J. A. *Large Ring Molecules*; Wiley: New York, 1996.
(3) Mcleish, T. *Science* **2002**, *297*, 2005–2006.
(4) Roovers, J. Organic Cyclic Polymers. In *Cyclic Polymers*, 2nd ed.; Semlyen, J. A., Ed.; Kluwer Academic Publishers: Dordrecht, 2000; pp 347−384.
(5) Mckenna, G. B.; Hostetter, B. J.; Hadjichristidis, N.; Fetters, L. J.; Plazek, D. J. *Macromolecules* **1989**, *22*, 1834–1852.
(6) Subramanian, G.; Shanbhag, S. *Phys. Rev. E* **2008**, *77*, 011801.
(7) Hur, K.; Winkler, R. G.; Yoon, D. Y. *Macromolecules* **2006**, *39*, 3975–3977.
(8) Jacobson, H.; Stockmayer, W. H. *J. Chem. Phys.* **1950**, *18*, 1600–1606.
(9) Endo, K. *Adv. Polym. Sci.* **2008**, *217*, 121–183.
(10) Geiser, D.; Höcker, H. *Macromolecules* **1980**, *13*, 653–656.
(11) Rique-Lurbet, L.; Schappacher, M.; Deffieux, A. *Macromolecules* **1994**, *27*, 6318–6324.
(12) Laurent, B. A.; Grayson, S. M. *J. Am. Chem. Soc.* **2006**, *128*, 4238–4239.
(13) Takano, A.; Kushida, Y.; Aoki, K.; Masuoka, K.; Hayashida, K.; Cho, D.; Kawaguchi, D.; Matsushita, Y. *Macromolecules* **2007**, *40*, 679–681.
(14) Mckenna, G. B.; Hadziioannou, G.; Lutz, P.; Hild, G.; Strazielle, C.; Straupe, C.; Rempp, P.; Kovacs, A. J. *Macromolecules* **1987**, *20*, 498–512.
(15) Wood, B. R.; Hodge, P.; Semlyen, J. A. *Polymer* **1993**, *34*, 3052–3058.
(16) Chisholm, M. H.; Gallucci, J. C.; Yin, H. *Proc. Natl. Acad. Sci. U.S.A.* **2006**, *103*, 15315–15320.
(17) Kudo, H.; Makino, S.; Kameyama, A.; Nishikubo, T. *Macromolecules* **2005**, *38*, 5964–5969.
(18) Bielawski, C. W.; Benitez, D.; Grubbs, R. H. *Science* **2002**, *297*, 2041–2044.
(19) Bielawski, C. W.; Benitez, D.; Grubbs, R. H. *J. Am. Chem. Soc.* **2003**, *125*, 8424–8425.
(20) Boydston, A. J.; Xia, Y.; Kornfield, J. A.; Gorodetskaya, I. A.; Grubbs, R. H. *J. Am. Chem. Soc.* **2008**, *130*, 12775–12782.

10.1021/ja809617v CCC: $40.75

Scheme 1. Proposed Zwitterionic Polymerization of Lactide To Generate Cyclic Polylactide

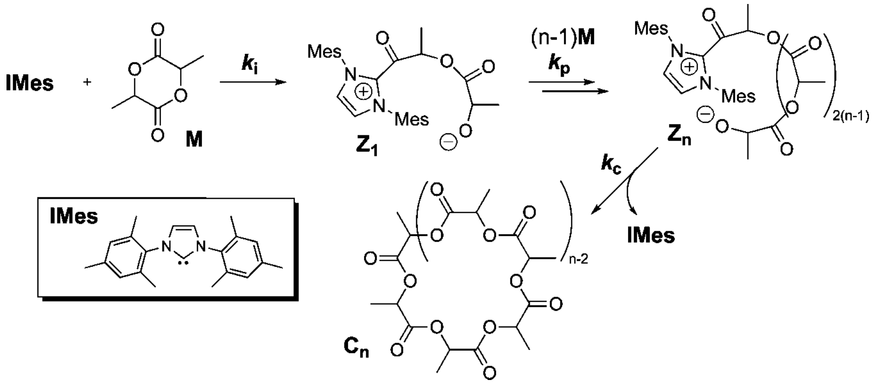

We recently reported the zwitterionic ring-opening polymerization of lactones by *N*-heterocyclic carbenes as a strategy to generate cyclic polyesters (Scheme 1).[23,24] Zwitterionic polymerizations are a class of ionic polymerizations where both the anion and the cation are attached to the same polymer chain.[25,26] Swarc had suggested as early as 1960 that zwitterionic polymerizations might lead to cyclic structures,[27] but only recently was this demonstrated experimentally.[23,24,28−30] In contrast to many other zwitterionic polymerizations,[25,26] the ring-opening polymerization of lactones by *N*-heterocyclic carbenes generates cyclic polylactones with high purity[31] and exceptional control of molecular weight and molecular weight distribution.[23,24] The cyclic structure of the products was confirmed by various experimental techniques including ^{1}H NMR spectroscopy, mass spectrometry, dynamic light scattering (DLS), and gel permeation chromatography (GPC).[23,24]

The zwitterionic polymerization of lactide exhibits several notable features: (1) the polymerization rates are rapid, reaching complete conversion within minutes, (2) relatively high molecular weight macrocycles are generated even at initial monomer concentrations $[M]_0 = 0.6-1.0$ M (in THF), (3) the molecular weight distributions are narrow (polydispersities (PDIs $= M_w/M_n) < 1.5$), and (4) the molecular weights ($M_n = 5-30$ kg/mol) increase with monomer conversion. The proposed mechanism for these reactions (Scheme 1) involves nucleophilic attack of the carbene initiator (I = IMes) to generate a zwitterionic intermediate (Z_1). Addition of monomers to the zwitterion (Z_1) leads to chain growth by generation of higher zwitterions (Z_n); macrocyclization of the zwitterions (Z_n) generates cyclic poly(lactide)s (C_n) with liberation of the carbene. This proposal provides a plausible explanation for the generation of cyclic polymers;[27] nevertheless, there are several features that are seemingly at odds with the observed polymerization behavior. In particular, the evolution of molecular weight with monomer conversion and the narrow molecular weight distributions are indicative of a chain-growth process with minimal chain transfer. If the rate of cyclization (R_c) were competitive with the rate of propagation (R_p), then cyclization would constitute a chain-transfer event as the liberated carbene should initiate the growth of another chain. Under these conditions, the molecular weights would be expected to remain constant with monomer conversion, and the molecular weight distribution should correspond to one predicted for chain growth with chain transfer, that is, $M_w/M_n = 2.0$.[32] As this is not observed experimentally, several unusual kinetic criteria need to be met to explain the observed polymerization behavior. In this Article, we detail our kinetic investigations of the zwitterionic polymerization of lactide that illuminate the kinetic features of these reactions that enable the generation of cyclic polyesters of defined molecular weight and molecular weight distribution.

Results and Discussion

The ring-opening polymerization of D,L-lactide (*rac*-lactide) in the presence of 1,3-dimesitylimidazol-2-ylidene (IMes; 0.5−1.0 mol % relative to monomer) is very fast, yielding cyclic poly(lactide)s within minutes at room temperature (Table 1).[23] The polymerization of D,L-lactide proceeded to 75% monomer conversion in 32 s with 0.5 mol % of IMes ($[M]_0 = 0.6$ M, $[M]_0/[I]_0 = 200$). The cyclic polylactides generated under these conditions have molecular weights ranging from $M_n = 5$ to 30 kg/mol with molecular weight distributions below $M_w/M_n = 1.5$ for monomer conversions less than 90%. The molecular weights of the resulting polymers increase with increasing monomer conversion (entries 1−4 and 5−8 in Table 1), but do not conform to simple predictions based on the monomer conversion and ratio $[M]_0/[I]_0$; for initial ratios of $[M]_0/[I]_0 = 100$, the experimental molecular weights are higher than those predicted, whereas for initial ratios of $[M]_0/[I]_0 = 200$, the experimental molecular weights are lower than those predicted. Attempts to generate cyclic polylactides with molecular weights higher than $M_n = 40$ kg/mol were unsuccessful.

As the molecular weights referenced to polystyrene typically overestimate the molecular weights for polylactides,[33,34] the

---

(21) Tezuka, Y.; Ohtsuka, T.; Adachi, K.; Komiya, R.; Ohno, N.; Okui, N. *Macromol. Rapid Commun.* **2008**, *29*, 1237–1241.

(22) Kricheldorf, H. R. *J. Polym. Sci., Part A: Polym. Chem.* **2004**, *42*, 4723–4742.

(23) Culkin, D. A.; Jeong, W.; Csihony, S.; Gomez, E. D.; Balsara, N. P.; Hedrick, J. L.; Waymouth, R. M. *Angew. Chem., Int. Ed.* **2007**, *46*, 2627–2630.

(24) Jeong, W.; Hedrick, J. L.; Waymouth, R. M. *J. Am. Chem. Soc.* **2007**, *129*, 8414–8415.

(25) Odian, G. *Principles of Polymerization*, 4th ed.; Wiley-Interscience: Hoboken, 2004.

(26) Johnston, D. S. *Adv. Polym. Sci.* **1982**, *42*, 51–106.

(27) Swarc, M. *Makromol. Chem.* **1960**, *35*, 132–158.

(28) Kricheldorf, H. R.; Von Lossow, C.; Schwarz, G. *J. Polym. Sci., Part A: Polym. Chem.* **2006**, *44*, 4680–4695.

(29) Kricheldorf, H. R.; Lomadze, N.; Schwarz, G. *Macromolecules* **2007**, *40*, 4859–4864.

(30) Kricheldorf, H. R.; Lomadze, N.; Schwarz, G. *Macromolecules* **2008**, *41*, 7812–7816.

(31) Under anhydrous polymerization conditions, we were unable to detect linear impurities by mass or NMR spectroscopy.

(32) Flory, P. J. *Principles of Polymer Chemistry*; Cornell University Press: Ithaca, 1953.

(33) Kowalski, A.; Duda, A.; Penczek, S. *Macromolecules* **1998**, *31*, 2114–2122.

Table 1. Selected Data for Cyclic Polylactides Prepared Using IMes

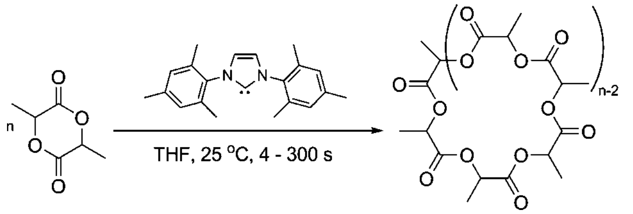

entry	time (s)	$[M]_0/[I]_0$[a]	conv (%)[b]	M_n (kg/mol)[c]	PDI[d]
1	4	100	13	5.3	1.27
2	8	100	42	9.8	1.27
3	16	100	73	13.3	1.25
4	24	100	85	16.1	1.30
5	8	200	23	7.8	1.31
6	16	200	48	12.5	1.25
7	24	200	67	15.8	1.24
8	32	200	75	16.8	1.28
9[e]	5	200	7	5.9	1.20
10[e]	12	200	30	11.7	1.14
11[e]	300	200	91	31.4	1.16
12[e]	15	30	92	28.6	1.24

[a] Initial monomer-to-initiator ratio; $[M]_0 = 0.6$ M. [b] Conversion determined by ^{1}H NMR spectroscopy. [c] Number average molecular weight; determined by gel permeation chromatography (GPC), calibrated with polystyrene standards. [d] Polydispersity index; determined by GPC, calibrated with polystyrene standards. [e] Sample purified by precipitation.

absolute molecular weights of samples 7 and 8 were determined by gel permeation chromatography (GPC) with a light scattering detector using an acetonitrile/dichloromethane mixture (4/1) as the solvent ($dn/dc = 0.112$).[35] The absolute weight-average molecular weights determined are $M_w = 13.9$ and 15.3 kg/mol, respectively, which are approximately 22% larger than the corrected molecular weights ($M_w = 11.4$ and 12.5 kg/mol) using the reported correction factor for linear poly(lactide)s.[33,34] As previously described, these results are a consequence of the smaller hydrodynamic volumes of the cyclic polyesters relative to their linear congeners.[23]

The ring-opening polymerization of lactide by the carbene IMes exhibits several characteristics of kinetically controlled living polymerization.[25,36] Polymerizations performed at $[M]_0 = 0.6$ M and $[I]_0 = 0.006$ M exhibit an increase of M_n with increasing conversion and yield polymers with narrow polydispersities ($M_w/M_n < 1.4$) for conversions less than 90% (Figure 1a). However, the polymerizations show some deviations from an ideal "living" behavior.[36] The polymerization rate does not exhibit simple first-order kinetics; the rate is accelerated at low monomer conversion and slows down at high monomer conversion (Figure 1b). In addition, the observed molecular weights do not conform to those predicted from the conversion and the ratio $[M]_0/[I]_0$; plots of the M_n versus monomer conversion extrapolate to a nonzero intercept at low monomer conversion (Figure 1a).

To reconcile the observed polymerization behavior with the proposed mechanism, in the following sections we consider a variety of kinetic models in an effort to illuminate the kinetic features of these zwitterionic polymerizations. The time evolution of the monomer concentration, molar mass, and PDI are analyzed by means of numerical and stochastic simulations for the initiation, propagation, termination, and chain-transfer steps.[36]

Model I: Slow Initiation and Fast Propagation. As the zwitterionic polymerization of lactide yields polymers with narrow PDIs and the molecular weights increase with monomer conversion, we initiated our kinetic analysis with the assumption that chain termination (cyclization) is much slower than propagation. The slight rate acceleration observed at the early stages of polymerization (Figure 1b) and the phenomenological nonzero intercept in the plot of molecular weight versus monomer conversion[36] (Figure 1a) suggest that the rate of initiation (formation of zwitterions) is slower than that of propagation. A kinetic scheme can be constructed analogous to the one for "living" polymerization with different rates of initiation (k_i) and propagation (k_p).[37,38] For the zwitterionic polymerization of lactide, the carbene is proposed to generate the propagating zwitterionic intermediate (Z_1).[23,24] A zwitterion (Z_n) undergoes the addition of monomer in the propagation steps. For simplicity, the rate coefficient of propagation is assumed to be independent of the size of the propagating species.

For Scheme 2, the rates of initiator and monomer conversion can be written as:

$$-\frac{d[I]}{dt} = k_i[I][M] \tag{1}$$

$$-\frac{d[M]}{dt} = k_i[I][M] + k_p([I]_0 - [I])[M] \tag{2}$$

Gold[37,38] first noted that the average degree of polymerization (DP) for this scheme is given by

$$\mathrm{DP} = \frac{[M]_0 - [M]}{[I]_0 - [I]} \tag{3}$$

$$= \left(1 - \frac{k_p}{k_i}\right) + \frac{k_p}{k_i}\cdot\left(\frac{[I]_0}{[I] - [I]_0}\right)\cdot\ln\left(\frac{[I]}{[I]_0}\right) \tag{4}$$

Experimentally, the accurate determination of [I] is cumbersome because of its low concentration (typically less than 0.01 M). To circumvent the need of evaluating [I], Hall rearranged the relevant equations into

$$\ln\left(\frac{1}{[I]_0}\cdot\frac{d\ln[M]}{dt} + k_p\right) = \ln(k_p - k_i) + k_i\int_0^t [M]\,dt \text{ when } k_p \geq k_i \tag{5}$$

in which there is no explicit term of [I].[39]

Pepper derived an equivalent of eq 5 without the integral of [M] as follows:

$$\ln\left(\frac{1}{k_p[I]_0}\cdot\frac{d\ln[M]}{dt} + 1\right) - \frac{1}{k_p[I]_0}\cdot\frac{d\ln[M]}{dt} = \frac{k_i}{k_p[I]_0}\cdot[M] + \frac{k_i}{k_p}\cdot\left(1 - \frac{[M]_0}{[I]_0}\right) + \ln\left(1 - \frac{k_i}{k_p}\right) \tag{6}$$

Equation 5 or 6 can be used to estimate the rate constants, k_p and k_i, by Hall's trial method.[39,40]

Fitting of the lactide polymerization data below 70% monomer conversion using eq 6 and Hall's trial method gives $k_p = 17$ (M^{-1} s^{-1}) and $k_i = 0.55$ (M^{-1} s^{-1}) (see Supporting

---

(34) Save, M.; Schappacher, M.; Soum, A. *Macromol. Chem. Phys.* **2002**, *203*, 889–899.
(35) Kang, S.; Zhang, G.; Aou, K.; Hsu, S. L.; Stidam, H. D. *J. Chem. Phys.* **2003**, *118*, 3430–3436.
(36) Matyjaszewski, K. *J. Phys. Org. Chem.* **1995**, *8*, 197–207.
(37) Gold, L. *J. Chem. Phys.* **1952**, *20*, 1651–1652.
(38) Gold, L. *J. Chem. Phys.* **1958**, *28*, 91–99.
(39) Beste, L. F.; Hall, H. K., Jr. *J. Phys. Chem.* **1964**, *68*, 269–274.
(40) Pepper, D. C. *Eur. Polym. J.* **1980**, *16*, 407–411.

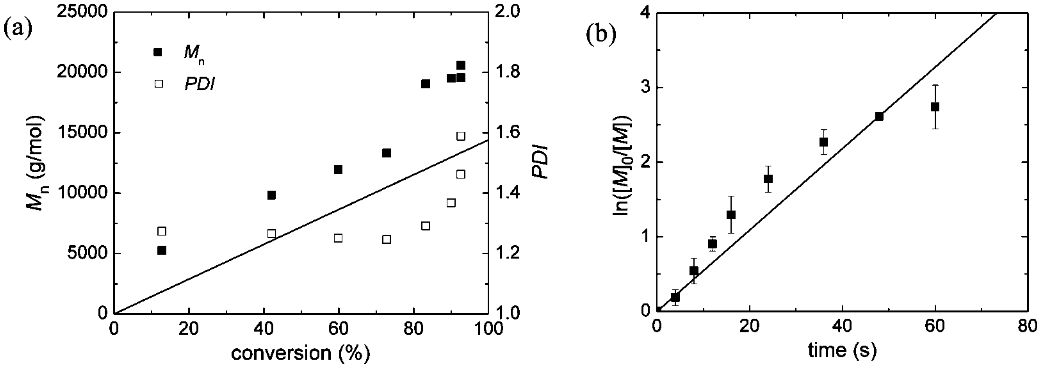

Figure 1. (a) Plots of M_n and PDI versus monomer conversion. The line is the theoretically predicted molecular weight for an ideal living polymerization. (b) First-order kinetic plot of the polymerization data at $[M]_0 = 0.6$ M and $[I]_0 = 0.006$ M. Each point is the average of three runs. The line is a linear fitting.

Scheme 2. "Living" Polymerization with Different Rate Constants of Initiation and Propagation

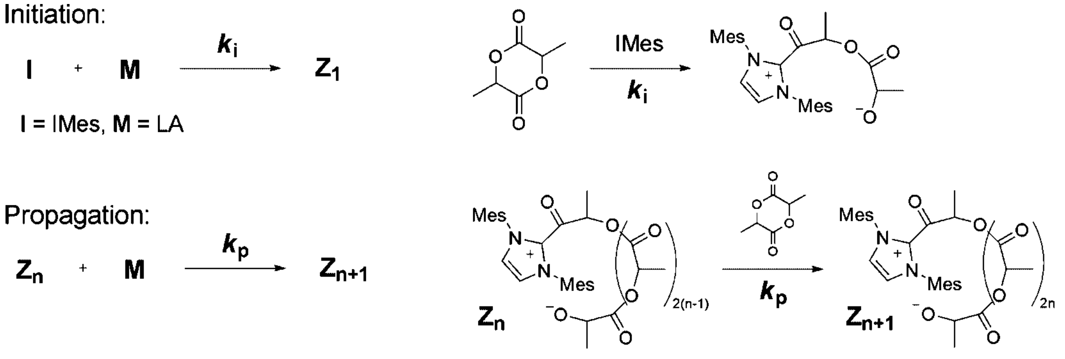

Information). Numerical fitting of the lactide polymerization data using the differential eqs 1 and 2 with a numerical solution of [I] provides $k_p = 17$ (M^{-1} s^{-1}) and $k_i = 0.57$ (M^{-1} s^{-1}).[41]

This analysis, which we reported previously,[23] provides a good fit to the time evolution of monomer conversion up to 70% conversion, but does not predict the decrease in rate at higher monomer conversion (Figure 2). In addition, while the rate constants $k_p = 17$ (M^{-1} s^{-1}) and $k_i = 0.57$ (M^{-1} s^{-1}) derived from polymerizations performed at $[M]_0 = 0.6$ M and $[I]_0 = 0.006$ M provide good fits for polymerizations performed at a lower carbene concentration ($[M]_0 = 0.6$ M and $[I]_0 = 0.003$ M), they significantly overestimate the rates observed at a lower monomer concentration ($[M]_0 = 0.3$ M and $[I]_0 = 0.003$ M).

Model II: Slow Initiation with Reversible Formation of the Initial Zwitterion and Fast Propagation. As the kinetics had suggested that the rate of initiation was slower than propagation, we sought an estimate of the rate of initiation from measurements of the initial rates. Kinetic plots utilizing the method of initial rates (Figure 3; Δ[M] versus time) reveal that the initial rates conform to:

$$(R_p)_0 \propto [M]^2[I] \tag{7}$$

The observed second-order dependence of $(R_p)_0$ on [M] implies that the initiation step is second order in monomer.[42] This can be accounted for if we assume that the initiation step involves the reversible formation of zwitterion Z_1 (Scheme 3).

Assuming a steady-state condition on $[Z_1]$, the initiation rate is described by

$$-\frac{d[I]}{dt} = \frac{k_1 k_2 [I][M]^2}{k_{-1} + k_2[M]} \tag{8}$$

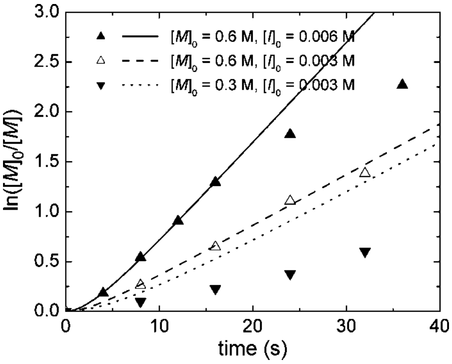

Figure 2. First-order kinetic plots of monomer conversion at some $[M]_0$'s and $[I]_0$'s. The lines are the numerical results based on the rate constants ($k_p = 17$ (M^{-1} s^{-1}) and $k_i = 0.57$ (M^{-1} s^{-1})) determined at $[M]_0 = 0.6$ M and $[I]_0 = 0.006$ M.

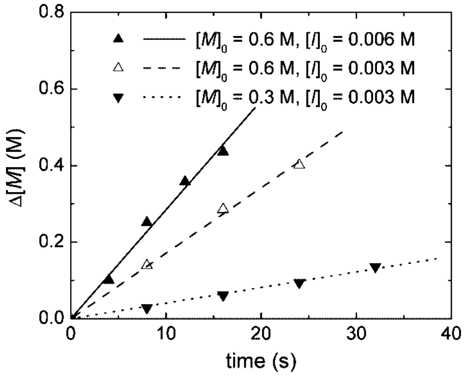

Figure 3. Plots of Δ[M] versus time. The lines are linear fittings.

Scheme 3. Initiation with the Reversible Formation of Zwitterion Z_1

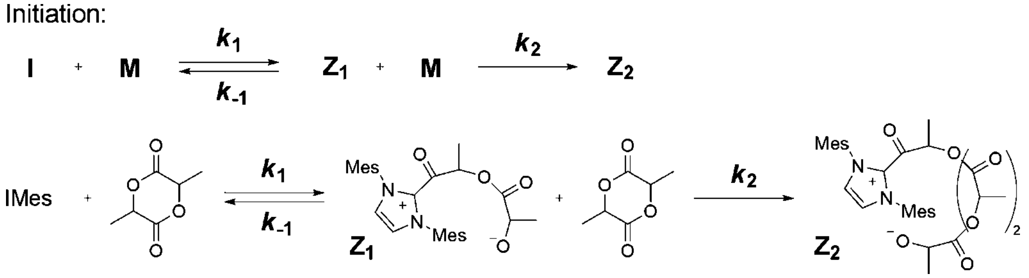

Scheme 4. Cyclization Reaction during Zwitterionic Polymerization

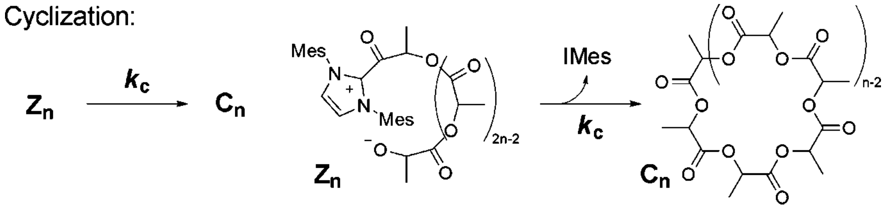

Scheme 5. Depropagation Reaction during Zwitterionic Polymerization

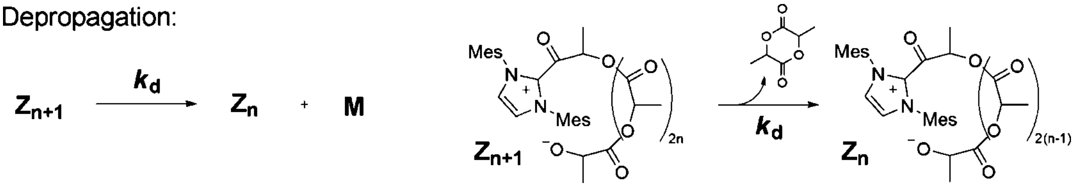

When k_{-1} is greater than k_2[M], eq 8 simplifies to:

$$-\frac{\mathrm{d}[\mathrm{I}]}{\mathrm{d}t} \cong \frac{k_1k_2[\mathrm{I}][\mathrm{M}]^2}{k_{-1}} \tag{9}$$

with

$$k_\mathrm{i} = \frac{k_1k_2}{k_{-1}} \tag{10}$$

Consequently, the rates of initiator and monomer conversion for Scheme 3 are written as

$$-\frac{\mathrm{d}[\mathrm{I}]}{\mathrm{d}t} = k_\mathrm{i}[\mathrm{I}][\mathrm{M}]^2 \tag{11}$$

$$-\frac{\mathrm{d}[\mathrm{M}]}{\mathrm{d}t} = 2k_\mathrm{i}[\mathrm{I}][\mathrm{M}]^2 + k_\mathrm{p}([\mathrm{I}]_0 - [\mathrm{I}])[\mathrm{M}] \tag{12}$$

which is consistent with the observed second-order dependence in [M] for the initial rates.

Numerical fitting of the lactide polymerization data at $[\mathrm{M}]_0 = 0.6$ M and $[\mathrm{I}]_0 = 0.006$ M below 70% conversion using eqs 11 and 12 yields estimates for $k_\mathrm{p} = 19.2$ ($\mathrm{M}^{-1}\ \mathrm{s}^{-1}$) and $k_\mathrm{i} = 0.788$ ($\mathrm{M}^{-2}\ \mathrm{s}^{-1}$). Numerical modeling with these rate constants gives better agreement with the experimental polymerization data at $[\mathrm{M}]_0 = 0.3$ M and $[\mathrm{I}]_0 = 0.003$ M (better than Figure 2), but the simulation results are still unsatisfactory (see Supporting Information) as they do not predict the decrease in rate at high monomer conversion and the molecular weights predicted using eq 3 of this model are much higher than observed experimentally (see Supporting Information). These discrepancies motivated further refinements in the kinetic model, as described below.

Model III: Slow Initiation with Reversible Formation of the Initial Zwitterion, Fast Propagation, Depropagation, and Cyclization. The observed decrease in the rate of polymerization at high monomer conversion (>70%) suggests a decrease in the number of propagating species at low [M] and consequently the presence of termination steps. Macrocyclization to liberate the cyclic polymer and the carbene initiator would decrease the concentration of propagating species ($\sum_n[\mathrm{Z}_n]$) under conditions where reinitiation is not competitive with cyclization. As the propagation rate is proportional to [M] and $\sum_n[\mathrm{Z}_n]$, and the cyclization rate is only proportional to $\sum_n[\mathrm{Z}_n]$, the cyclization reaction would be expected to exert a more significant influence on the overall kinetics at high monomer conversion (low [M]) (Scheme 4).

Assuming that cyclization is unimolecular and its rate constant (k_c) is independent of the size of the propagating species, then the rates of initiator conversion can be written as:

$$-\frac{\mathrm{d}[\mathrm{I}]}{\mathrm{d}t} = k_\mathrm{i}[\mathrm{I}][\mathrm{M}]^2 - k_\mathrm{c}([\mathrm{I}]_0 - [\mathrm{I}]) \tag{13}$$

At high monomer conversion, the system approaches equilibrium between polymerization and depolymerization. The relatively modest enthalpy of polymerization ($\Delta H_\mathrm{p}^0 = -29$ kJ mol^{-1}) and negative entropy of polymerization of lactide ($\Delta S_\mathrm{p}^0 = -41$ J $\mathrm{mol}^{-1}\ \mathrm{K}^{-1}$) result in a nonzero equilibrium concentra-

---

(41) The small difference in k_i is likely due to an error in estimating d ln[M]/dt in Hall's trial method.

(42) Another possibility is that propagation is second order in [M]. Yet this possibility is ruled out by unreasonably high molecular weights predicted on the basis of this model (see Supporting Information).

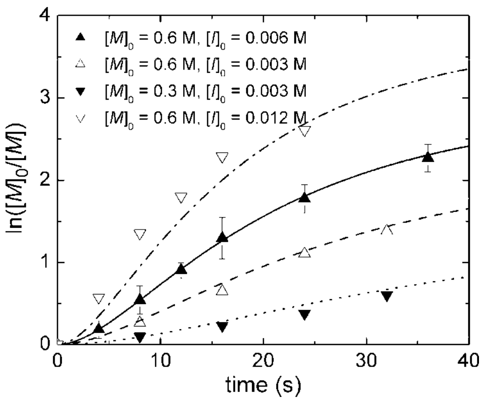

Figure 4. Plots of logarithm of $[M]_0/[M]$ versus time at some $[M]_0$'s and $[I]_0$'s. The lines are the numerical results based on the rate constants determined at $[M]_0 = 0.6$ M and $[I]_0 = 0.006$ M.

tion of monomer ($[M]_e = 0.014$ M at 25 °C in 1,4-dioxane),[43] suggesting that the rate of depropagation cannot be ignored at high monomer conversion.[25] If this depropagation step (Scheme 5) is taken into account, the effective rate constant for propagation (k_p^{eff}) can be written as

$$k_p^{eff} = k_p - \frac{k_d}{[M]} \qquad (14)$$

$$-\frac{d[M]}{dt} = 2k_i[I][M]^2 + k_{eff}([I]_0 - [I])[M] \qquad (15)$$

If depropagation is considered, eq 16 is given by substituting eq 14 into eq 15:

$$-\frac{d[M]}{dt} = 2k_i[I][M]^2 + (k_p[M] - k_d)([I]_0 - [I]) \qquad (16)$$

Numerical fitting of the lactide polymerization data at $[M]_0 = 0.6$ M and $[I]_0 = 0.006$ M (Figure 4, up to more than 90% conversion) to the differential eqs 13 and 16 provides good agreement with the kinetic data at various concentrations and yields the estimates for the rate constants: $k_i = 0.274$ (M^{-2} s^{-1}), $k_p = 48.7$ (M^{-1} s^{-1}), $k_d = 0.208$ (s^{-1}), and $k_c = 0.0575$ (s^{-1}).

This kinetic model illuminates a number of unique features of these ring-opening polymerization reactions. First, the polymerization rates are very high; the rate constant for propagation ($k_p = 49$ M^{-1} s^{-1}) is on the order of enzymatic rate constants for ring-opening polymerization of lactide ($k_{cat} = 2-225$ (s^{-1}))[44] and faster than that for metal alkoxides (NaOR,[45] $k_p = 0.7$ (M^{-1} s^{-1}) at 80 °C; ZnOR,[46] $k_p = 2.2$ (M^{-1} s^{-1})). Second, the narrow PDIs are a consequence of the high rate of propagation relative to cyclization ($R_p/R_c = k_p[M]/k_c = 850[M]$) and the inefficiency of reinitiation by the carbene initiator liberated upon cyclization, due to the low rate of initiation that is second order in [M].

The proposed mechanistic model is further tested by Monte Carlo simulations to predict the molecular weights and molecular weight distributions.[47−49] The rate constants derived from numerical fitting of differential eqs 13 and 16 were used as inputs for stochastic kinetic simulations of 100 000 chains to evaluate the evolution of molecular weight and PDI as a function of time (see Supporting Information). The validity of the simulations was checked by reproducing the numerical data of polymerization kinetics under various conditions. These simulations capture some of the key experimental observations found in the evolution of molecular weight and PDI (Figures 5 and 6). The molecular weight distributions remain narrow (PDIs < 1.5) for conversion less than 90%. The molecular weights increase with increasing monomer conversion, and exhibit a nonzero intercept, but are relatively insensitive to the ratio of $[M]_0/[I]_0$. All of these findings could be understood on the basis of the proposed mechanistic model involving slow initiation, fast propagation, and competitive depropagation and cyclization at high monomer conversion.

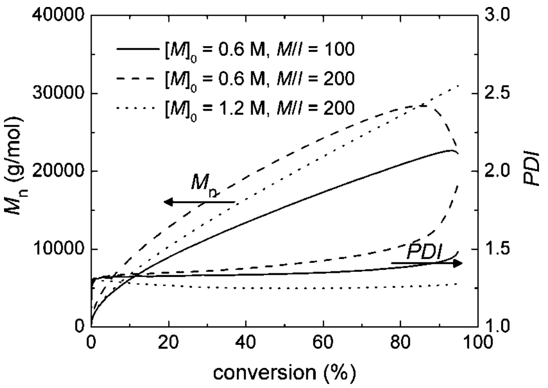

Figure 5. Plots of M_n and PDI versus monomer conversion at some $[M]_0$'s and $[I]_0$'s predicted on the basis of the proposed mechanistic model ($k_i = 0.274$ (M^{-2} s^{-1}), $k_p = 48.7$ (M^{-1} s^{-1}), $k_d = 0.208$ (s^{-1}), and $k_c = 0.0575$ (s^{-1})).

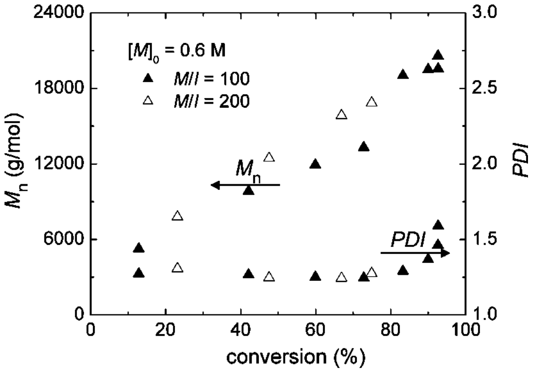

Figure 6. Plots of experimental M_n and PDI versus monomer conversion at some $[M]_0$'s and $[I]_0$'s.

The simulations provide important insights as they enable an estimation of the amount of free carbenes (I), active zwitterions (Z_n), and "dead" chains (C_n)[50] at any monomer conversion (given initial inputs of $[M]_0$, $[I]_0$, and rate constants).

---

(43) Duda, A.; Florjanczyk, Z.; Hofman, A.; Slomkowski, S.; Penczek, S. *Macromolecules* **1990**, *23*, 1640–1646.

(44) Van Der Mee, L.; Helmich, F.; De Bruijin, R.; Vekemans, J. A. J. M.; Palmans, A. R. A.; Meijer, E. W. *Macromolecules* **2006**, *39*, 5021–5027.

(45) Baran, J.; Duda, A.; Kowalski, A.; Szymanski, R.; Penczek, S. *Macromol. Symp.* **1997**, *123*, 93–101.

(46) Williams, C. K.; Breyfogle, L. E.; Choi, S. K.; Nam, W.; Young, V. G.; Hillmyer, M. A.; Tolman, W. B. *J. Am. Chem. Soc.* **2003**, *125*, 11350–11359.

(47) Matyjaszewski, K.; Szymanski, R.; Teodorescu, M. *Macromolecules* **1994**, *27*, 7565–7574.

(48) Szymanski, R. *Macromol. Theory Simul.* **1998**, *7*, 27–39.

(49) Szymanski, R.; Baran, J. *Macromol. Theory Simul.* **2002**, *11*, 836–844.

(50) It is possible that the carbene can react with cyclized chains to regenerate macro-zwitterionic species. We currently have no evidence either for or against this hypothesis, and further studies are underway to test whether cyclized chains can be reinitiated for further chain growth.

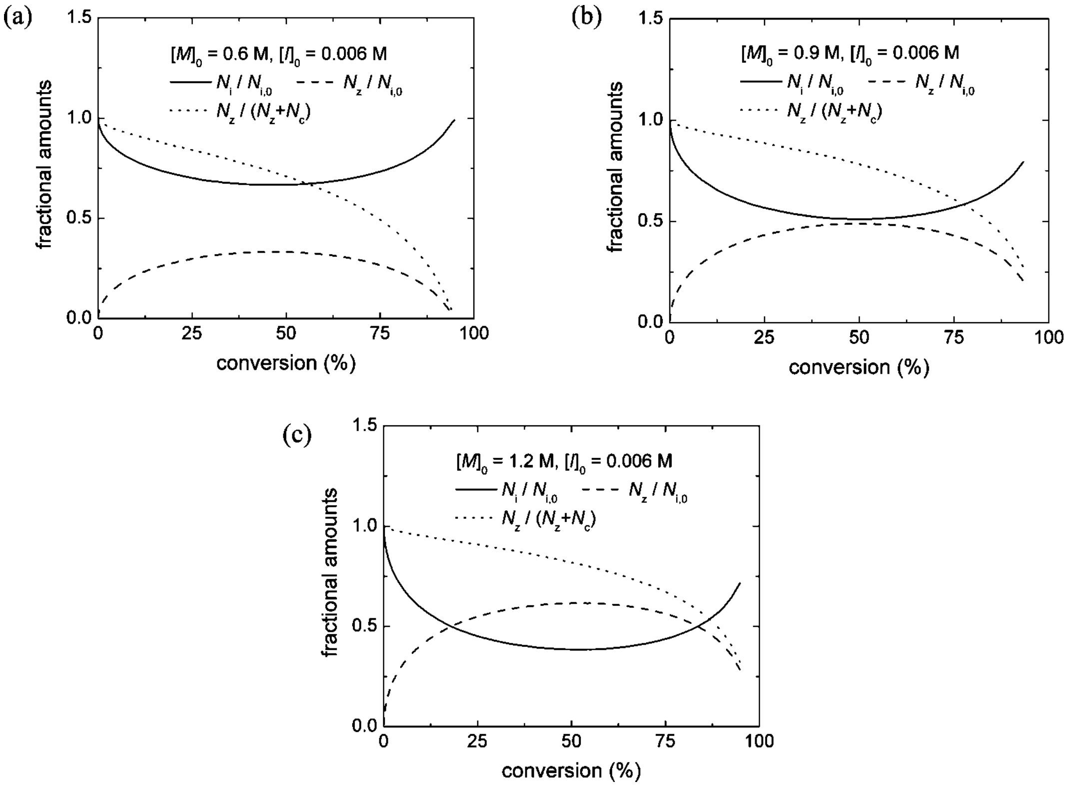

Figure 7. Stochastic simulations of polymerization kinetics at (a) $[\mathrm{M}]_0 = 0.6$ M and $[\mathrm{I}]_0 = 0.006$ M, (b) $[\mathrm{M}]_0 = 0.9$ M and $[\mathrm{I}]_0 = 0.006$ M, and (c) $[\mathrm{M}]_0 = 1.2$ M and $[\mathrm{I}]_0 = 0.006$ M. $N_{\mathrm{i},0}$ is the initial number of initiators, and N_i, N_z, and N_c are the number of initiators, zwitterions, and cyclized chains, respectively.

Scheme 6. Sequential Polymerization of Lactide

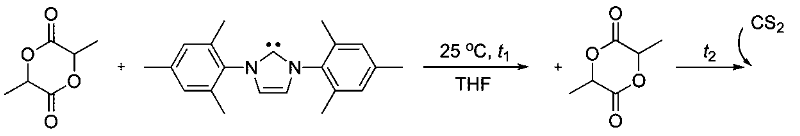

(a) $[M]_{0,1st} = 0.6$ M, $[I]_0 = 0.006$ M, $t_1 = 60$ s
(b) $[M]_{0,1st} = 0.9$ M, $[I]_0 = 0.006$ M, $t_1 = 10$ s

(a) $[M]_{0,2nd} = 1.2$ M, $t_2 = 30$ s
(b) $[M]_{0,2nd} = 0.9$ M, $t_2 = 30$ s

For example, kinetic simulations for polymerizations at $[\mathrm{M}]_0 = 0.6$ M and $[\mathrm{I}]_0 = 0.006$ M reveal that even at 50% monomer conversion, a significant fraction of initiators still remain ($N_\mathrm{i}/N_{\mathrm{i},0} = [\mathrm{I}]/[\mathrm{I}]_0 = 0.67$; $N_{\mathrm{i},0}$ is the initial number of initiators, and N_i is the number of initiators) due to the slow initiation relative to propagation (the solid line in Figure 7a). At higher monomer conversion, the fraction of initiators increases due to liberation of the carbene initiator by macrocyclization. Importantly, as initiation at high monomer conversion is suppressed because of low [M] and the second-order dependence of initiation on [M], initiators start accumulating after 50% monomer conversion.

The observation that this system exhibits some characteristics of "living polymerization" but deviates from living behavior can be readily understood by considering the evolution of the amount of active species during the polymerization (the broken lines in Figure 7a−c). The fraction of active zwitterions ($N_\mathrm{z}/N_{\mathrm{i},0}$) increases initially and reaches a maximum (for example, 0.33 in Figure 7a and 0.62 in Figure 7c at 50% monomer conversion). Subsequently, the fraction of active zwitterions $N_\mathrm{z}/N_{\mathrm{i},0}$ decreases upon cyclization of the macrozwitterions. The molecular weight is formally given by eq 3, the ratio of the concentration of converted monomer ($[\mathrm{M}]_0 - [\mathrm{M}]$) to the concentration of active species ($[\mathrm{I}]_0 - [\mathrm{I}]$). Because $[\mathrm{I}]_0 - [\mathrm{I}]$ changes with time, the evolution of molecular weight with monomer conversion would not be expected to follow that for a "living" polymerization where $[\mathrm{I}]_0 - [\mathrm{I}]$ is constant and typically equal to $[\mathrm{I}]_0$.[25,36−38] The observed increase in molecular weight with monomer conversion is a consequence of the slow cyclization (as compared to propagation) and the relatively constant $[\mathrm{I}]_0 - [\mathrm{I}]$ between 25% and 75% monomer conversion.

The simulation results for polymerizations at higher $[\mathrm{M}]_0$ (Figure 7b and c) clearly show an important consequence of the second-order dependence of initiation on [M]: Polymerization at a higher initial monomer concentration generates a larger fractional amount of active species. In the polymerizations at $[\mathrm{M}]_0 = 1.2$ M and $[\mathrm{I}]_0 = 0.006$ M (Figure 7c), up to 65% initiators are converted to active zwitterions. At 90% monomer conversion, the fraction of active species ($N_\mathrm{z}/N_{\mathrm{i},0}$) is 0.41 for polymerizations at $[\mathrm{M}]_0 = 1.2$ M and $[\mathrm{I}]_0 = 0.006$ M, whereas $N_\mathrm{z}/N_{\mathrm{i},0}$ is only 0.11 for polymerizations at $[\mathrm{M}]_0 = 0.6$ M and $[\mathrm{I}]_0 = 0.006$ M.

The simulations help define the kinetic conditions under which chain extension of the active zwitterions might be expected. To test these predictions, chain-extension experiments were carried out by adding a second charge of monomer during the course of the polymerization (Scheme 6).

An initial polymerization of *rac*-lactide (0.70 mmol) was performed in a THF solution (1.16 mL, $[\mathrm{M}]_0 = 0.6$ M, and $[\mathrm{I}]_0$

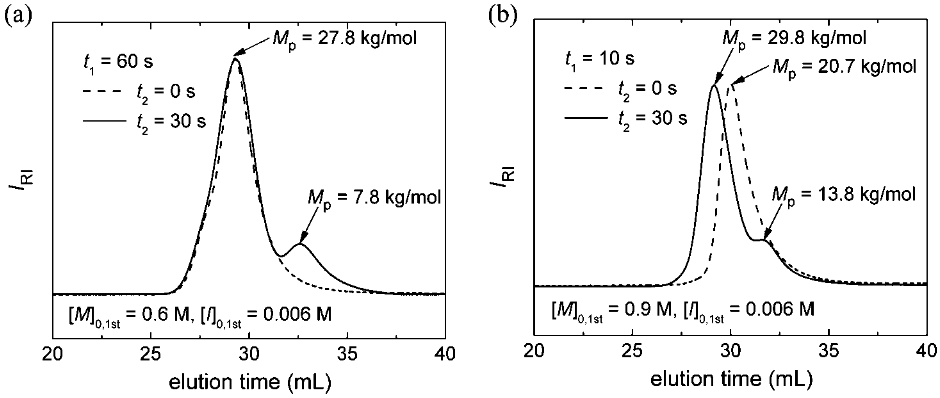

Figure 8. GPC traces of crude products from the sequential polymerizations (a) at $[M]_{0,\text{first}} = 0.6$ M and $[I]_{0,\text{first}} = 0.006$ M ($t_1 = 60$ s, $t_2 = 30$ s (solid); $t_1 = 60$ s, $t_2 = 0$ s (dashed)), and (b) at $[M]_{0,\text{first}} = 0.9$ M and $[I]_{0,\text{first}} = 0.006$ M ($t_1 = 10$ s, $t_2 = 30$ s (solid); $t_1 = 10$ s, $t_2 = 0$ s (dashed)).

= 0.006 M). After $t_1 = 60$ s (94% monomer conversion), a 1.2 M THF solution of *rac*-lactide (1 mL) was added, and then stirring was continued for an additional 30 s (t_2) before being quenched with CS_2. It was observed that only 30% of monomer was converted in the second polymerization. Analysis of the crude samples by GPC reveals that the addition of more monomer causes the formation of a small shoulder in the low molecular weight regime, but no discernible change in the main peak (Figure 8a). The stochastic simulations based on the proposed mechanistic model predict $N_i/N_{i,0} = 0.95$, $N_z/N_{i,0} = 0.05$, and $N_c/N_{i,0} = 0.55$ for the first polymerization after $t_1 = 60$ s (94% monomer conversion, Figure 7a). Notably, the simulations suggest that the "dead" chains cyclized during the first polymerization constitute more than 90% of the main peak at 94% monomer conversion. Also, the experimentally observed most probable molecular weight (M_p) of the second shoulder peak is 7.8 kg/mol, which is close to that for the polymerization at low monomer conversion (entry 5 in Table 1). These experimental and simulation results implicate that the addition of additional monomer after 94% conversion results in reinitiation rather than chain extension and that the shoulder observed at lower molecular weight (Figure 8a) corresponds to reinitiated polymers.

In contrast, if the initial polymerization is carried out at higher monomer concentration and the second monomer charge is added at a lower conversion, chain extension is observed. For example, polymerization of *rac*-lactide (1.04 mmol) in THF at higher monomer concentration (1.15 mL, $[M]_0 = 0.9$ M, and $[I]_0 = 0.006$ M) for 10 s proceeded to 59% conversion (Figure 8b). The same polymerization is carried out, but a second monomer charge (1.15 mL of a 0.9 M THF solution) is added after $t_1 = 10$ s, and the reaction was continued for an additional 30 s (t_2) before being quenched with CS_2. Analysis of the crude samples by ^{1}H NMR spectroscopy reveals that 64% of monomer was converted during the polymerizations (49% of monomer was converted in the second polymerization; see Supporting Information). GPC traces of the crude samples show that the addition of more monomer causes an increase in the molecular weight of the main peak and the formation of a small shoulder in the low molecular weight regime (Figure 8b). These results indicate that under these conditions, chain extension of the propagating zwitterions occurs, but is accompanied by some reinitiation of polymerization by the residual carbenes in solution. These observations are consistent with the simulations (Figure 7b) that predict a significant fraction of both active zwitterions ($N_z/N_{i,0} = 0.48$) and carbenes ($N_i/N_{i,0} = 0.52$) at 59% conversion. The shoulder observed at $M_p = 13.8$ g/mol (Figure 8b) is likely due to reinitiation from the carbenes in solution, but may also include the "dead" chains cyclized during the first polymerization ($N_c/N_{i,0} = 0.18$).

While it is likely that the kinetic simulations do not represent all of the kinetic features of these polymerizations, the agreement between the predictions of the kinetic simulations and the chain-extension experiments provides strong support for the kinetic model and illuminates the factors that define the kinetic lifetime of the active zwitterions.

Conclusion

In summary, the zwitterionic ring-opening polymerization of lactide provides a fast and efficient method for the synthesis of cyclic polylactides of defined molecular weight and molecular weight distribution. Kinetic and mechanistic investigations reveal that the rate of initiation is second order in [M] and slower than propagation, and the rate of propagation is faster than that of cyclization. The proposed mechanistic model provides key insights into the unusual features observed in these polymerizations. Of particular significance is the origin of the narrow molecular weight distributions. In the proposed model, the observed molecular weight distributions versus monomer conversion are explained by the fast propagation relative to the macrocyclization and the slow initiation at high monomer conversion due to its second-order dependence on [M]. The cyclization, although slow relative to the propagation, places limits on the molecular weights that can be achieved. Consequently, the proposed model guides further investigations on the development of new NHC initiators that enable polymerization with faster initiation and slower cyclization as compared to IMes. The proposed mechanistic framework sets the stage for further optimization of these zwitterionic polymerizations to generate large ring polyesters of defined molecular weight.

Acknowledgment. We gratefully acknowledge support from the NSF Center on Polymeric Interfaces and Macromolecular Assemblies (CPIMA: NSF-DMR-0213618) and NSF-GOALI Grant NSF-CHE-0645891. We thank Purac for a generous donation of lactide. Dr. Szilárd Csihony is acknowledged for his initial discovery of the zwitterionic polymerization of lactide. E.J.S. is grateful for the Samsung Scholarship from the Samsung Foundation of Culture.

Supporting Information Available: Experimental procedures and simulation methods. This material is available free of charge via the Internet at http://pubs.acs.org.

JA809617V